Applied Catalysis B: Environmental 90 (2009) 360–367

Contents lists available at ScienceDirect

Applied Catalysis B: Environmental

journal homepage: www.elsevier.com/locate/apcatb

Non-thermal plasma-assisted catalytic NO_x storage over $Pt/Ba/Al_2O_3$ at low temperatures

Junhua Li [a,c,*], Woo Huang Goh [b], Xuechang Yang [b], Ralph T. Yang [c]

[a] Department of Environment Science and Engineering, Tsinghua University, Beijing 100084, China
[b] Department of Electrical Engineering, Tsinghua University, Beijing 100084, China
[c] Department of Chemical Engineering, University of Michigan, Ann Arbor, MI 48109-2136, USA

ARTICLE INFO

Article history:
Received 16 January 2009
Received in revised form 27 February 2009
Accepted 16 March 2009
Available online 25 March 2009

Keywords:
Nitric oxide
NSR
Lean NO_x trap
Non-thermal plasma
Dielectric barrier discharge
$Pt/Ba/Al_2O_3$
Adsorption
Oxidation

ABSTRACT

NO_x storage performances have been investigated on a $Pt/Ba/Al_2O_3$ catalyst by comparison using two types of non-thermal plasma (NTP) reactor: the "PDC system" reactor and the "PFC system" reactor. In the PDC system, the catalyst was placed in the discharge space and was activated by the plasma directly, whereas in the PFC system, the plasma reactor was followed by the catalyst. The results showed that the NO_x storage capacity (NSC) of the $Pt/Ba/Al_2O_3$ catalyst was significantly enhanced by the non-thermal plasma in the PDC and PFC system, and the PDC system exhibited better promotional effect than the PFC system in the temperature range of 100–300 °C. The NSC of the catalyst was increased with the increase of the input energy density both in the PDC and PFC system due to the higher NO oxidation at higher input energy density. It was also found that the ionic wind induced by plasma in the PDC system enhanced the quantity of the NO adsorbed onto the catalyst surface and therefore could react with the O-radical to form more NO_2, and thus promote the formation of nitrate on the catalyst.

1. Introduction

In recent years, the diesel and lean-burn gasoline engines have attracted much attention for their remarkable potential to improve the fuel economy and reduce the greenhouse gas CO_2 emission compared with the conventional stoichiometric gasoline engines. However, the conventional three-way catalysts cannot reduce NO_x effectively in a lean exhaust due to the high oxygen level. One potential solution is the use of NO_x storage and reduction (NSR) or the so-called "lean NO_x trap" (LNT), which was first conceived by Toyota [1,2]. The typical NSR catalysts consist of three principal components: a precious metal (PM) for oxidation and reduction of NO_x (e.g. Pt, Rh), a storage material (e.g. an alkaline or alkaline earth metal oxides), and a high surface area support material (e.g. alumina).

Although NSR catalyst is emerging as a commercially viable approach for lean NO_x reduction, however, it has not been widely used in diesel vehicles due to the narrow temperature window. For example, the exhaust gas temperature of a light-duty diesel vehicle driving under the Federal Test Procedure (FTP) is typically less than 200 °C, while the operation temperature window of the conventional NSR ranges from 200 to 500 °C [3].

It is reported that the NO_x storage is a critical step of the NSR process, and the adsorption of NO_2 is more facile than that of NO over the NSR catalyst [4–13]. However, the NO_x storage capacity (NSC) is limited by the low NO oxidation rate at relatively low temperature. Therefore, to enhance the activation of NO in the exhaust to NO_2 and other radicals at low temperature has become an important step to substantially increase the performance of the NSR catalyst.

To achieve effective NO oxidation activities lower than 200 °C, the non-thermal plasma (NTP) is found to be a promising choice since the NO can be effectively oxidized to NO_2 by non-thermal plasma process under the condition of excess oxygen [14–16]. Therefore, the main idea of this work is to enhance the NO_x storage capacity of $Pt/Ba/Al_2O_3$ catalyst by comparison using two types of plasma-catalyst combined method: single-stage plasma-driven catalyst (PDC), and two-stage plasma-followed-by catalyst (PFC), and then to investigate the NO_x storage process through FT-IR.

* Corresponding author at: Department of Environment Science and Engineering, Tsinghua University, Beijing 100084, China. Tel.: +86 10 62782030; fax: +86 10 62785687.
E-mail address: lijunhua@tsinghua.edu.cn (J. Li).

0926-3373/$ – see front matter © 2009 Elsevier B.V. All rights reserved.
doi:10.1016/j.apcatb.2009.03.017

2. Experimental

2.1. Catalyst preparation

The $Pt/Ba/Al_2O_3$ catalyst (1/20/100 w/w) in these experiments was prepared by incipient wetness impregnation of alumina in two sequential steps as follows. An Al_2O_3 carrier (230 m^2/g) was firstly impregnated with a solution of $H_2PtCl_6.6H_2O$ with an appropriate concentration. After drying in air for 12 h at 80 °C and calcinations at 500 °C for 5 h, batches of this catalyst were impregnated with a $Ba(CH_3COO)_2$. The impregnated sample was initially dried in air for 12 h at 80 °C and then calcined at 500 °C for 5 h. The specific surface area of $Pt/Ba/Al_2O_3$ catalyst obtained was 136 m^2/g.

2.2. Plasma reactor

For laboratory experiments, the non-thermal plasma was obtained in a coaxial cylinder-type dielectric barrier discharge (DBD) reactor by using a quartz tube (inner diameter 22 mm, outer diameter 25 mm) as a dielectric barrier between the inner high voltage electrode (stainless steel tube, outer diameter 16 mm) and a grounded electrode (stainless steel mesh) on the outer wall. The plasma reactor was energized by AC high voltage power at 50 Hz.

The measurement of the discharge power was carried out by using voltage–charge (V–Q) Lissajous figure method [17]. The applied voltage was measured with a 1000:1 high voltage probe and the charge Q was determined by measuring the voltage across the 33 nF capacitor connected to the ground line of the plasma reactor in series, with a 10:1 voltage probe. From this, the specific input energy density was calculated with the following relations:

$$\text{Specific input energy density (J/L)} = \frac{\text{Discharge power (W)}}{\text{Gas flow rate (L/min)}} \times 60.$$

2.3. NO_x adsorption/desorption

The thermal NO_x adsorption experiments were conducted by comparison using catalyst-only, single-stage plasma-driven catalyst (PDC) system, and two-stage plasma-followed-by catalyst (PFC) system with simulated exhaust gases under atmospheric pressure. The catalysts were placed directly in the discharge space during the PDC system, whereas the catalysts were placed in a quartz tube reactor with an internal diameter of 6 mm downstream from the plasma reactor during the PFC system. The schematic overview of these two kinds of reactors was given in Scheme 1.

Prior to the NO_x adsorption experiment, the catalyst sample was pretreated in a flow of 8% O_2, N_2 at 500 °C for 30 min and then cooled down to the storage temperature. Thereafter, the sample was exposed to a 500 ppm NO, 8% O_2 and N_2 mixture at gas hourly space velocity (GHSV) of about 35,000 h^{-1} for 1 h. During the adsorption, concentrations of NO_x were measured by an NO–NO_2–NO_x analyzer (Thermal Environmental Instruments, Model 42C).

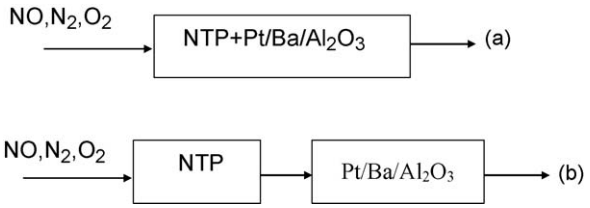

Scheme 1. Schematic overview of two types of plasma-catalyst configurations. (a) PDC system: the catalyst was placed in the discharge space; (b) PFC system: the plasma reactor was followed by the catalyst.

After the NO_x adsorption, the sample was purged with N_2 until no NO_x concentration was detected in order to remove the weakly adsorbed species at the adsorption temperature. The temperature programmed desorption (TPD) measurements were then carried out from 80 °C to 600 °C with a heating rate of 10 °C/min in flowing N_2. Concentrations of NO_x in the outlet stream were monitored, and the amount of desorbed NO_x was thus calculated as the NO_x storage capacity (NSC) of the catalyst.

2.4. Diffuse reflectance FT-IR spectroscopy

The diffuse reflectance FT-IR (DRIFTS) measurements were carried out in situ in a high-temperature cell fitted with ZnSe windows. The samples were finely ground, placed directly to a ceramic crucible and manually pressed. The feed gas streamed into the cell at a total flow rate of 100 mL/min with or without non-thermal plasma pre-treatment in PFC system. Prior to analysis, the $Pt/Ba/Al_2O_3$ samples were pretreated at 500 °C in a mixture of N_2 and 8% O_2 for 30 min, then in N_2 for 30 min to remove surface residues. Background spectra were collected after dwelling for 30 min at a given temperature, except when specially noted. All spectra were measured with 4 cm^{-1} resolution using a liquid nitrogen cooled MCT detector of the Nicolet Nexus 870-FT-IR.

3. Results

3.1. The NO_x storage capacity

The outlet NO_x concentrations during a storage experiment for the NSR catalyst-only and two plasma-catalyst combined systems are shown in Fig. 1. In these experiments, the storage temperature was set at 100 °C and the specific input energy density for PFC and PDC was set at 190 J/L. It can be observed that the catalyst stored more NO_x when using PFC and PDC methods although the NO_x breakthrough time was a bit shorter than the catalyst-only. In addition, the PDC showed a much better NO_x storage capability than the PFC at this low temperature. At the storage time of 60 min, the outlet NO_2/NO ratio recorded at the catalyst-only, PFC and PDC system was 0.03, 0.06 and 0.24, respectively. This indicated that the PFC and PDC had a higher NO oxidation activity than the catalyst-only.

Fig. 2 compares the NO_x storage capacity of the $Pt/Ba/Al_2O_3$ catalyst-only with the PFC and PDC at various temperatures from 100 °C to 300 °C. In these experiments, the specific input energy density for PFC and PDC was also set at 190 J/L. The results showed that NO_x storage capacity of the catalyst was clearly enhanced by introducing plasma to the catalyst. In particular, the NSC of catalyst

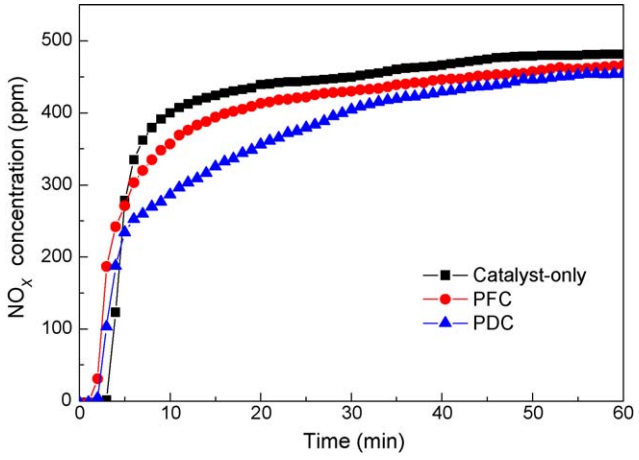

Fig. 1. NO_x adsorption profiles at 100 °C. Energy density of plasma: 190 J/L.

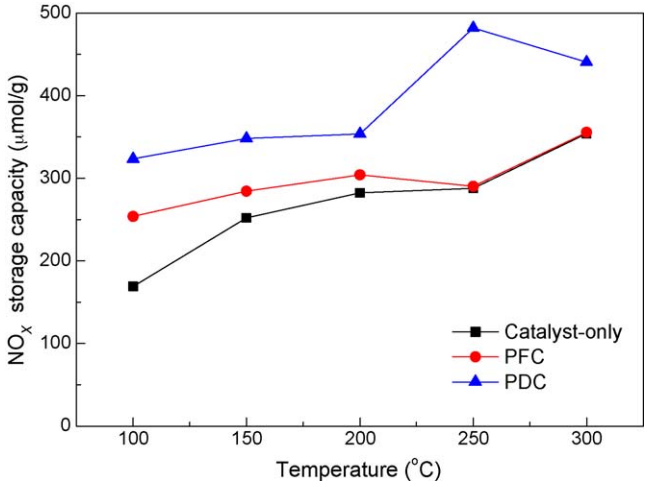

Fig. 2. The NO_x storage capacity of the catalyst-only, PFC and PDC system at different adsorption temperature. Energy density of plasma: 190 J/L.

in PFC system increased by 50.2%, 12.9%, 7.7%, 0.8% and 0.5% at 100 °C, 150 °C, 200 °C, 250 °C and 300 °C, respectively, as compared with the catalyst-only. It can be seen that in the PFC system there was no significant enhancement at temperature higher than 200 °C. However, in contrast with PFC system, the NSC of catalyst in PDC system increased by 91.3%, 38.2%, 25.2%, 67.9% and 24.5% at the temperature of 100 °C, 150 °C, 200 °C, 250 °C and 300 °C, respectively, as compared with the catalyst-only. These results indicated a better "synergistic effect" was presented between the catalyst and plasma in the PDC system.

The outlet NO_2/NO ratios in the three cases are listed in Table 1. It can be observed that the NO_2/NO ratio of the PFC was higher than the catalyst-only from 100 °C to 200 °C, but it was then almost the same at above 200 °C. In contrast, the NO_2/NO ratios of the PDC were much higher than both cases from 100 °C to 300 °C.

3.2. NO_x desorption

Temperature-programmed desorption under nitrogen was carried out over catalyst only, PFC and PDC after NO_x adsorption at various temperatures from 100 °C to 300 °C, up to 60 min. The results of the TPD experiments are shown in Fig. 3.

Obviously, the NO desorption followed a two-step process in the case of 500 ppm NO + 8% O_2 adsorption at 100 °C. In particular, the low-temperature NO desorption peak occurred at 270–300 °C while the high-temperature NO peak occurred at 500–520 °C (Fig. 3A). It can be also noted in Fig. 3A that PFC had larger NO desorption peak than the catalyst-only at high-temperature whereas the PDC had larger NO desorption peaks both at low-temperature and high-temperature. From Fig. 3B, it can be seen that the NO_2 desorption for the catalyst-only and PFC system also followed a two-step process. In particular, the low-temperature NO_2 peak occurred at around 225 °C while the high-temperature NO_2 peak occurred at around 500 °C. Although the concentration of desorbed NO_2 was low (below 30 ppm), but it still can be observed that the amount of desorbed NO_2 for the PFC and PDC was greater than the catalyst-only as shown in Fig. 3B.

In the case of NO_x adsorption at 150 °C, there were also two distinct NO desorption peaks occurred at 250–280 °C and 480–510 °C in all three cases (Fig. 3C). However, the PDC and PFC exhibited different feature with respect to catalyst-only, with respect to the higher amount of NO_x released at high-temperature compared to that of released at low-temperature. It can be seen that the high-temperature NO peaks of the PFC and PDC were larger and broader than catalyst-only but the low-temperature NO peaks had became lower than the catalyst-only. Further, the high-temperature NO peak showed maxima slightly shifted toward lower temperatures (~30 °C) in the case of PDC as compared with the maxima of the catalyst-only. As shown in Fig. 3D, there were also two NO_2 desorption peaks occurred in all cases with NO_2 concentration being less than 50 ppm. It can also be observed that the PFC and PDC had larger NO_2 desorption peaks than the catalyst-only.

Fig. 3E illustrates the desorption progress of NO from catalysts that previously adsorbed NO_x at 200 °C. It can be observed that there were still two NO desorption peaks occurred at 280–290 °C and 480–510 °C. However, the low-temperature NO peak amplitude of PFC and PDC had became much lower while the high-temperature NO peak amplitude had became much larger compared to the case of NO_x adsorption at 150 °C. As can see from Fig. 3F, the NO_2 desorption peak of the PDC had became much greater than the PFC and catalyst-only.

Fig. 3G and H shows the TPD results with NO_x adsorption at 250 °C. It can be seen from Fig. 3G that there was a weak low-temperature NO peak occurred at 300 °C and a high-temperature peak occurred at 510 °C in the case of catalyst-only while there was only high-temperature peak occurred at 510 °C and 490 °C in the cases of PFC and PDC, respectively. Significantly, the PDC had broader and more intense desorption band of NO and NO_2 (Fig. 3H) than the catalyst-only and PFC.

As can see from Fig. 3I, there was only high-temperature NO peak occurred in all three cases after NO_x adsorption at 300 °C. It can be also noted that the PDC had broader NO desorption band and the high-temperature peak had also slightly shifted toward lower temperatures (~30 °C) compared to the catalyst-only and PFC. Furthermore, the total amount of NO_2 desorbed for the PDC was almost the same with the PFC and catalyst-only as depicted in Fig. 3J.

The amounts of NO_x desorbed at low-temperature (below 350 °C, denoted as D_L) and at high-temperature (350 °C to 600 °C, denoted as D_H), as a percentage of the total desorbed NO_x (denoted as D_T) were listed in Table 2. As shown in Table 2 and Fig. 3, it can be observed that the NO_x desorbed at low-temperature became lesser whereas the NO_x desorbed at high-temperature became much greater with the increase of NO_x adsorption temperature in all three cases. In particular, in the case of catalyst-only, the D_L was greater than D_H when the adsorption temperature was below

Table 1
The outlet NO_2/NO ratios during NO_x adsorption at different temperature.

T (°C)	Catalyst-only NO_2/NO ratio	PFC* NO_2/NO ratio	PDC* NO_2/NO ratio
100	0.03	0.06	0.24
150	0.03	0.06	0.11
200	0.08	0.09	0.14
250	0.13	0.12	0.26
300	0.24	0.24	0.45

* Energy density for PDC and PFC: 190 J/L.

Table 2
The ratios of the NO_x desorption in two steps.

T (°C)	Catalyst-only		PFC*		PDC*	
	D_L/D_T (%)	D_H/D_T (%)	D_L/D_T (%)	D_H/D_T (%)	D_L/D_T (%)	D_H/D_T (%)
100	72.94	27.06	44.83	55.17	44.11	55.89
150	61.69	38.31	37.76	62.24	31.82	68.18
200	42.77	57.23	27.66	72.34	4.53	95.47
250	2.89	97.11	2.50	97.50	0	100
300	0	100	0	100	0	100

* Energy density for PDC and PFC: 190 J/L.

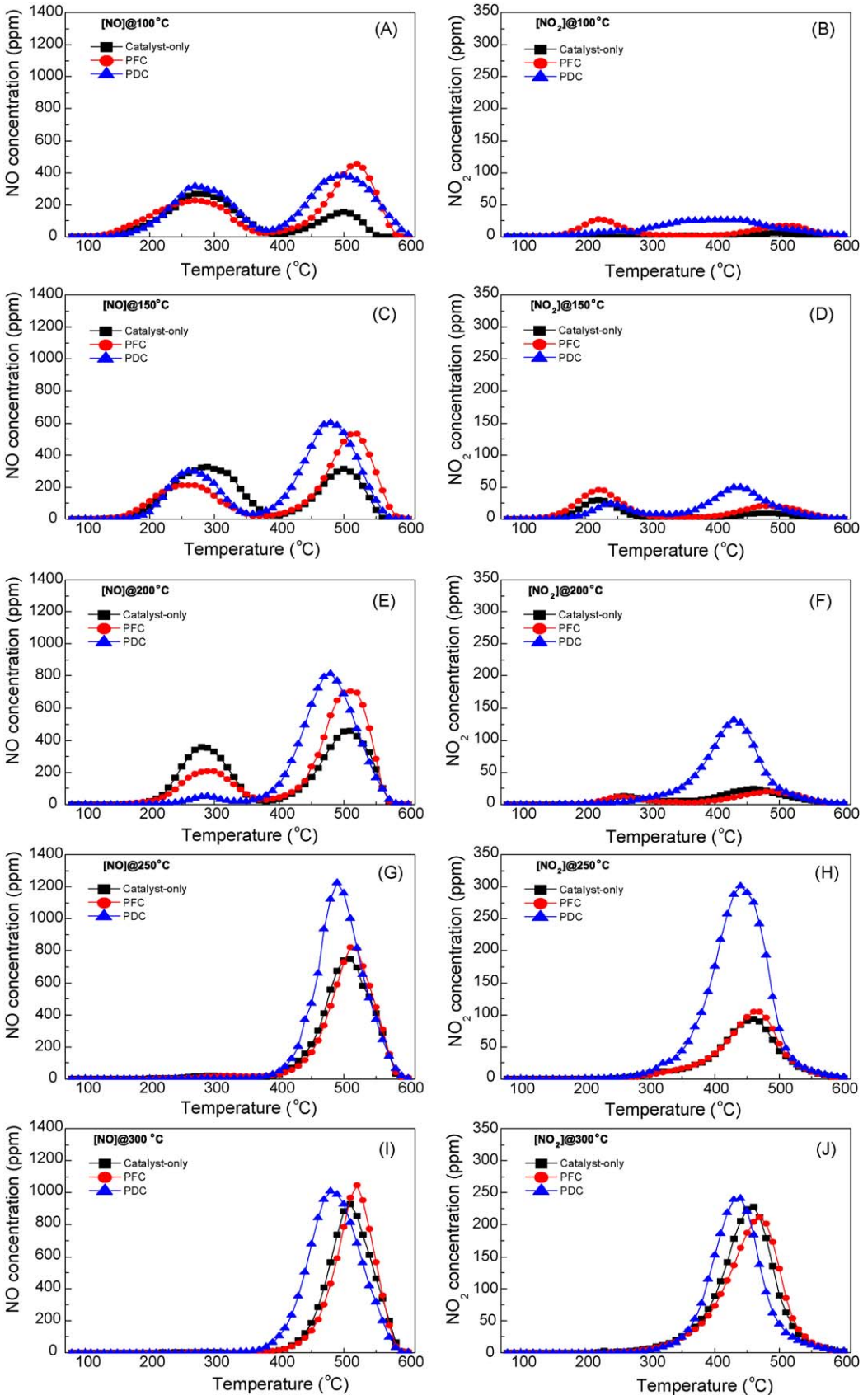

Fig. 3. NO_x–TPD spectra of the catalyst-only, PFC, PDC that previously adsorbed. 500 ppm NO + 8% O_2 at 100 °C (A and B), 150 °C (C and D), 200 °C (E and F), 250 °C (G and H) and 300 °C (I and J). Energy density of plasma: 190 J/L.

200 °C. With an increase of adsorption temperature to 200 °C, the D_H became much greater than D_L and at higher adsorption temperature (300 °C) there was only NO_x desorption at high-temperature. In the case of PFC, it can be noted that the D_H was greater than D_L at the adsorption temperature start from 100 °C to 300 °C and the D_L had disappeared at higher adsorption temperature (>250 °C). For PDC, the D_H was also greater than D_L from 100 °C to 300 °C. However, the D_L had nearly disappeared (D_L/D_T: 4.53%) at 200 °C. It can be also noted in Table 2 that the D_L/D_T (%) was systematically decreasing in the order of catalyst-only > PFC > PDC while the D_H/D_T (%) was systematically increasing in the order of PDC > PFC > catalyst-only.

From the experimental results, it is clearly that the plasma in the PDC and PFC can enhance the amount of NO_x-adsorbed species which will desorb at high-temperature during the TPD experiment.

3.3. DRIFTS spectra

3.3.1. NO_x adsorption

In situ diffuse reflectance FT-IR spectra of catalyst-only and PFC system during adsorption of 500 ppm NO in the presence of 8% oxygen at 100 °C are shown in Fig. 4A and B, respectively. As shown in Fig. 4A, after 5 min of exposure a broad band was observed at 1232 cm^{-1}, together with weak bands at 1325 cm^{-1} and 1627 cm^{-1}. The broad band at 1232 cm^{-1} can be assigned to bridging nitrite [18] whereas the weak bands at 1325 cm^{-1} and 1627 cm^{-1} can be assigned to the monodentate nitrate and physical adsorption of NO_2, respectively [19,20]. With further NO/O_2 exposure, all bands grew in intensities and a new weak band–which can be assigned to bidentate nitrate [20] appeared at approximately 1402 cm^{-1}. After 60 min of NO/O_2 adsorption, the band at 1232 cm^{-1} (bridging nitrite) became the most pronounced band in the entire spectrum.

When compared to the corresponding spectra obtained with the catalyst-only and the catalyst in the PFC system shown in Fig. 4A and B, it became apparent that there was synergistic effect between the plasma pre-treatment and the catalyst since the intensity of the nitrate band at 1325 cm^{-1}, 1402 cm^{-1} and the physical adsorption of NO_2 at 1627 cm^{-1} were much higher after 60 min of NO/O_2 adsorption with the presence of plasma.

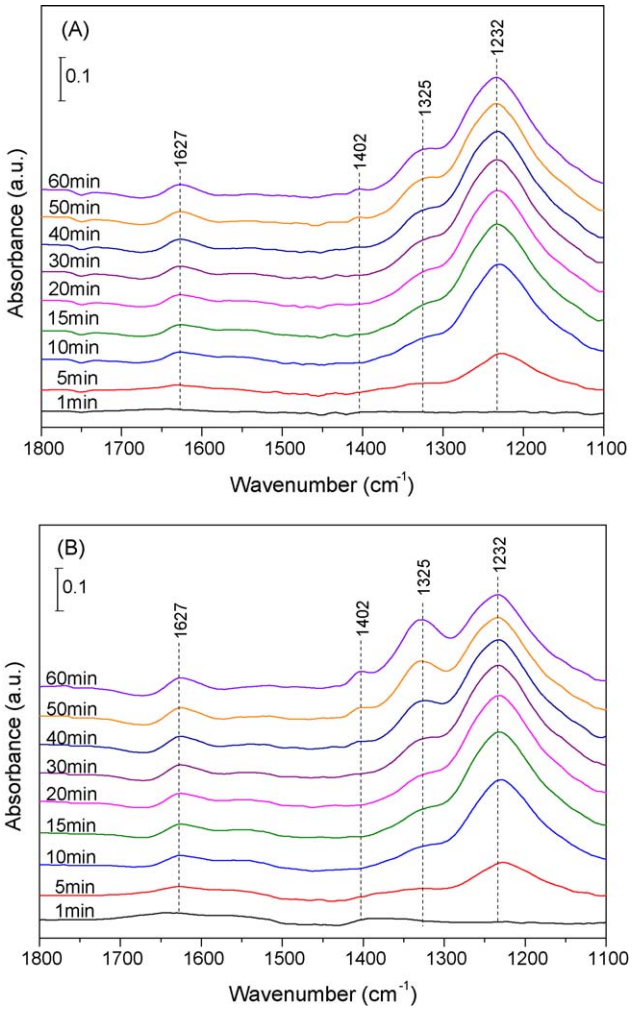

Fig. 4. DRIFTS spectra of the adsorption of 500 ppm NO + 8% O_2 on: (A) catalyst-only and (B) catalyst in PFC system at 100 °C.

3.3.2. Thermal desorption of adsorbed NO_x species

Further information about the nature of the surface species observed in the NO/O_2 adsorption experiments was gained through the thermal desorption studies. After exposure to 500 ppm NO + 8% O_2 at 100 °C for 60 min, the $Pt/Ba/Al_2O_3$ catalyst in the PFC system was heated linearly from 100 °C to 600 °C at a heating rate of 10 °C/min in flowing N_2, and the resulting IR spectra were shown in Fig. 5. It can be seen that the physical adsorption of NO_2 with characteristic band at 1627 cm^{-1} remained on the surface until 250 °C. The band at 1232 cm^{-1}, attributed to bridging nitrite, continuously decreased and vanished at around 350 °C. It should be noted that at 250 °C a new band at 1545 cm^{-1} – which can be assigned to bridging nitrate [19] – was observed to grow in intensity with the decrease of bridging nitrite. This indicated that a portion of the bridging nitrite species may be converted to the bridging nitrate species during the thermal desorption. As the temperature was increased to 400 °C, the monodentate nitrate (1325 cm^{-1}), bidentate nitrate (1402 cm^{-1}) and the bridging nitrate (1545 cm^{-1}) bands started to decrease in intensity and completely disappeared at 600 °C.

3.4. Effect of gas species ($NO/O_2/N_2$ or NO/N_2) in adsorption

The effect of gas species in adsorption ($NO/O_2/N_2$ or NO/N_2) on NO_x desorbed was examined with TPD method. The adsorption condition was as follows: for $NO/O_2/N_2$ was 500 ppm NO, 8% O_2 and N_2 as balance gas, for NO/N_2 was 500 ppm NO and N_2 as balance gas, flow rate = 400 mL/min, temperature = 100 °C, adsorption time = 60 min, specific input energy density = 190 J/L.

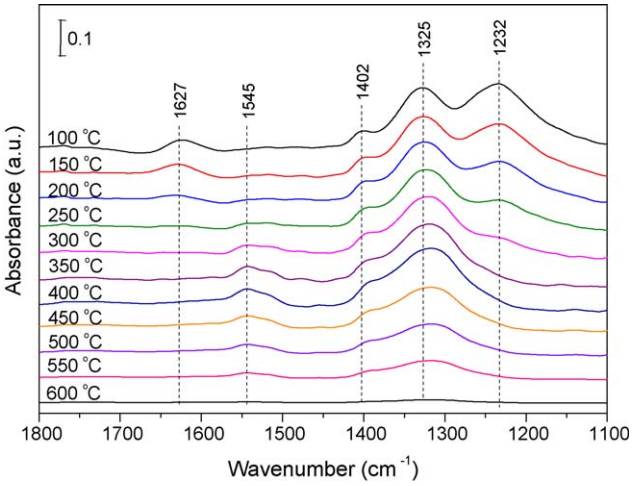

Fig. 5. DRIFTS spectra collected during the thermal desorption of NO_x adsorbed onto the catalyst in the PFC system.

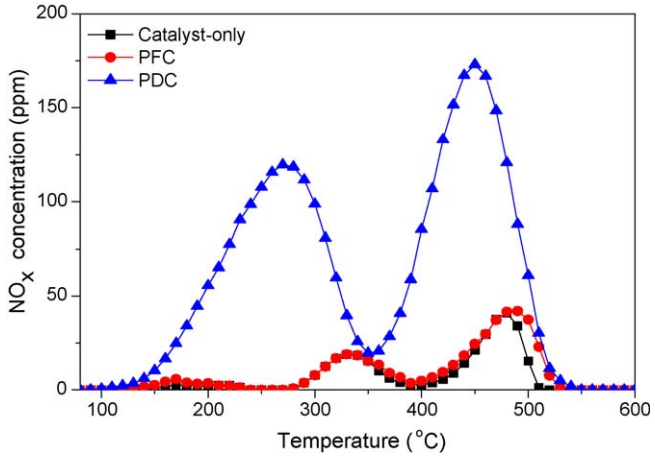

Fig. 6. The NO_x–TPD spectra of the $Pt/Ba/Al_2O_3$ for the different adsorption process after 500 ppm NO adsorption on the pre-oxidized sample at 100 °C.

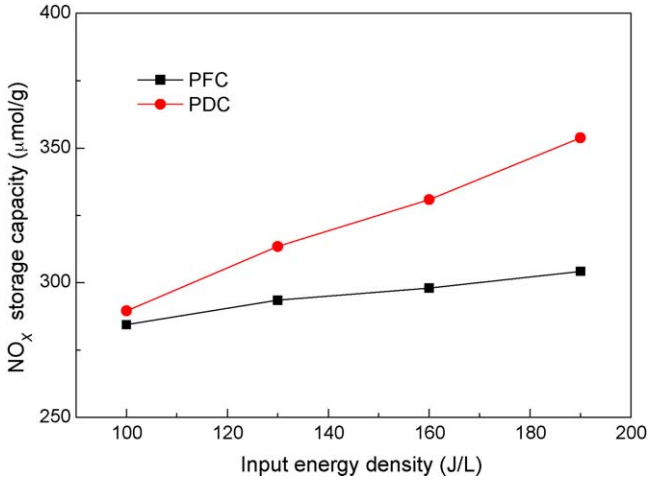

Fig. 7. The NO_x storage capacity of the PFC and PDC system for different input energy density at 200 °C.

The TPD results of $NO/O_2/N_2$ adsorption are shown in Fig. 3A and B, while the TPD results of NO/N_2 adsorption are shown in Fig. 6. The NSC of the catalyst only, PFC and PDC in two different adsorption conditions is shown in Table 3. Compare with the results shown in Fig. 3A and B, Fig. 6 and Table 3, it can be observed that the NSC in the NO/N_2 condition was much less than in the $NO/O_2/N_2$ condition. However, it can be noted that the catalyst in the PDC system could adsorb significant amounts of NO even in the absence of oxygen whereas the NSC of the catalyst in the PFC system was almost the same with the catalyst-only. This indicated that the plasma pre-treatment in the PFC system could not enhance the NSC of the catalyst without the presence of oxygen whereas the plasma in the PDC system could enhance the direct adsorption of NO on the catalyst.

3.5. Effect of the different input energy density

The experimental was carried out over PFC and PDC with 500 ppm NO + 8% O_2 adsorption at 200 °C. The results in Fig. 7 showed that the NO_x storage capacity of the PFC and PDC system increased with the increase of the input energy density. In particular, with the increase of the input energy density from 100 J/L to 190 J/L, the NO_x storage capacity of the PFC increased from 284 μmol/g to 304 μmol/g whereas the PDC increased from 290 μmol/g to 354 μmol/g.

The TPD spectrum of NO_x for the PFC and PDC that previously applied different input energy density during NO_x adsorption are shown in Fig. 8. Obviously, it can be seen from Fig. 8A that with the increase of the input energy density, the intensity of the low-temperature peak became much lower whereas the high-temperature peak became much larger in the case of PDC. Furthermore, the high-temperature peak had also slightly shifted toward lower temperatures with the increase of the input energy density. It can be also observed in Fig. 8B that the TPD spectrum of the PFC had similar feature with the PDC. However, the changes of the peak intensity with the increase of the input energy density were not so obvious as compared with PDC. Furthermore, the high-temperature peak of the PFC would not shift toward lower temperatures with the increase of the input energy density.

Table 3
The NSC of catalyst-only, PFC, and PDC in different condition: $NO/O_2/N_2$ and NO/N_2 adsorption at 100 °C.

System	$NO/O_2/N_2$ NSC (μmol/g)	NO/N_2 NSC (μmol/g)
Catalyst-only	169.1	12.5
PFC*	253.9	16.3
PDC*	323.5	108.1

* Energy density for PDC and PFC: 190 J/L.

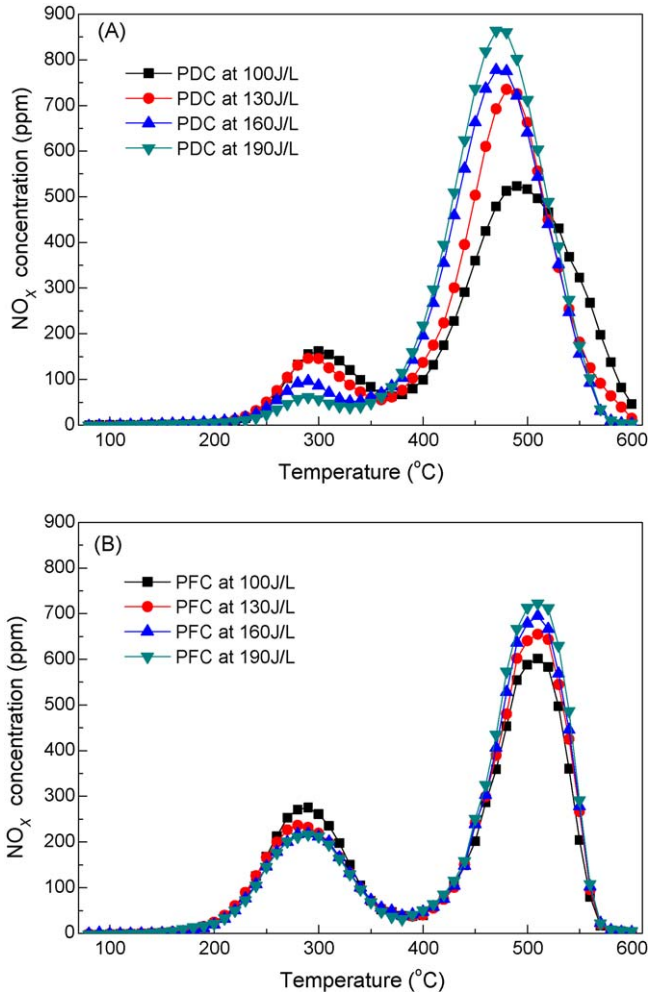

Fig. 8. The NO_x–TPD spectra of the $Pt/Ba/Al_2O_3$ at different input energy density for (A) PDC system and (B) PFC system.

4. Discussion

Data reported in Fig. 2 shows clearly that the NO_x adsorption can be enhanced efficiently by introducing the non-thermal plasma to the catalyst through PFC and PDC system. It is because the NO can be oxidized to NO_2 by the non-thermal plasma and the NO_2 can be adsorbed on the catalyst surface with lower adsorption energy than NO. However, there is difference between PFC system and PDC system since the PDC system has exhibited a higher NO_x adsorption capacity than PFC system. In our belief, it can be attributed to the ability of enhance the NO to adsorb on the catalyst surface as shown in Fig. 6. It is reported that electric discharge created on ionic wind [21–24], which will induce gas flow between the electrical poles at the considerable velocity of a few milliseconds. Thus, we believe that the diffusion of gas molecules as well as the interaction between gas molecules and catalyst surface can be improved by an ionic wind. Therefore, more NO can be adsorbed on the catalyst surface. It is also believed that the O-radical which is formed by the electron collisions with O_2 in the plasma may also be able to be adsorbed onto the catalyst surface by the ionic wind [24], and may react with the adsorbed NO to form NO_2.

From the experimental results shown in Fig. 2, it can be seen that the NSC enhancement in the PFC system decrease with increasing temperature. We suggest this phenomenon is attributable to the lower oxidation efficiency of NO at higher temperature and can be explained by the rates of the relevant reactions shown as follows [25–28]:

$$NO + O \rightarrow NO_2 \quad k_1 = 5.0 \times 10^{-33} \exp\left(\frac{900}{T}\right) \tag{1}$$

$$NO + O_3 \rightarrow NO_2 + O_2 \quad k_2 = 1.0 \times 10^{-31} \left(\frac{300}{T}\right)^{1.6} \tag{2}$$

$$O + O_2 \rightarrow O_3 \quad k_3 = 5.6 \times 10^{-34} \left(\frac{300}{T}\right)^{2.23} \tag{3}$$

$$O + O_3 \rightarrow 2O_2 \quad k_4 = 8.0 \times 10^{-12} \exp\left(\frac{-2060}{T}\right) \tag{4}$$

It has been reported that ozone plays an important role in the oxidation of NO at room temperature [28]. However, as can be seen in reactions (3) and (4), generation of ozone decreases much with increasing temperature and the decomposition into molecular oxygen becomes significant as the temperature increases. As a result, reaction (2) cannot contribute to the oxidation of NO at high temperatures, and therefore the NO oxidation rate is lowered. Furthermore, the NO_2 may also convert back to NO by the O-radical ($NO_2 + O \rightarrow NO + O_2$) [25,29]. Consequently, there is no significant synergistic effect between plasma pre-treatment and catalyst at higher temperatures.

Comparing with the desorption temperature in the TPD spectra (Fig. 3A and B) and the DRIFTS spectra of the thermal desorption experiment (Fig. 5), we suggest that the low-temperature NO and NO_2 peak of the TPD spectra can be attributed to the decomposition of the nitrite species and desorption of the physical adsorbed NO_2, respectively, while the high-temperature NO and NO_2 peak can be attributed to decomposition of the nitrate species. The attribution for this species is in agreement with the literature [18,30,31,5,32,33]. It has also reported that the decomposition of the barium nitrates and nitrates is likely via the following reactions [34]:

$$Ba(NO_2)_2 \rightarrow BaO + 2NO + 0.5O_2 \tag{5}$$

$$Ba(NO_3)_2 \rightarrow BaO + 2NO + 1.5O_2 \tag{6}$$

$$Ba(NO_3)_2 \rightarrow BaO + 2NO_2 + O_2 \tag{7}$$

Thus, from the TPD spectra shown in Fig. 3 and the ratio data shown in Table 2, it is clear that the non-thermal plasma in the PFC and PDC system can enhance more nitrates to be formed on the catalyst as compare with the catalyst-only. However, it is believe that the PDC system can enhance more nitrates to be formed on the catalyst than the PFC system at the adsorption of above 200 °C since the amount of the desorbed NO_2 of the PDC system is found to be much greater than PFC system during the TPD experiments.

Generalizing all the results presented above and combining with the catalyst-only mechanism proposed by Epling et al. [33], Lietti et al. [31] and Fridell et al. [35], the mechanism of NO_x storage in the PFC and PDC system may be the following:

For PFC system:

$$O_{2(g)} \xrightarrow{plasma} 2O* \tag{8}$$

$$NO_{(g)} + O* \xrightarrow{plasma} NO_{2(g)} \tag{9}$$

$$NO_{2(g)} \xrightarrow{catalyst} NO_{2(ad)} \tag{10}$$

$$NO_{(g)} \xrightarrow{catalyst} NO_{(ad)} \tag{11}$$

$$NO_{(ad)} + O*_{(ad)} \xrightarrow{catalyst} NO_{2(ad)} \tag{12}$$

$$BaO + 2NO_{(ad)} + O*_{(ad)} \xrightarrow{catalyst} Ba(NO_2)_2 \tag{13}$$

$$Ba(NO_2)_2 + 2O*_{(ad)} \xrightarrow{catalyst} Ba(NO_3)_2 \tag{14}$$

$$BaO + 2NO_{(ad)} + 3O*_{(ad)} \xrightarrow{catalyst} Ba(NO_3)_2 \tag{15}$$

$$BaO + 2NO_{2(ad)} + O*_{(ad)} \xrightarrow{catalyst} Ba(NO_3)_2 \tag{16}$$

where g denotes as gaseous phase, * denotes as excited radical and ad denotes adsorption onto the catalyst surface.

For PDC system:

$$O_{2(g)} \xrightarrow{plasma} 2O* \tag{17}$$

$$NO_{(g)} + O* \xrightarrow{plasma} NO_{2(g)} \tag{18}$$

$$O_{2(g)} \xrightarrow{plasma} 2O*_{(ad)} \tag{19}$$

$$NO_{(g)} \xrightarrow{plasma} NO_{(ad)} \tag{20}$$

$$NO_{(ad)} + O*_{(ad)} \xrightarrow{catalyst} NO_{2(ad)} \tag{21}$$

$$NO_{2(g)} \xrightarrow{catalyst} NO_{2(ad)} \tag{22}$$

$$NO_{(g)} \xrightarrow{catalyst} NO_{(ad)} \tag{23}$$

$$BaO + 2NO_{(ad)} + O*_{(ad)} \xrightarrow{catalyst} Ba(NO_2)_2 \tag{24}$$

$$Ba(NO_2)_2 + 2O*_{(ad)} \xrightarrow{catalyst} Ba(NO_3)_2 \tag{25}$$

$$BaO + 2NO_{(ad)} + 3O*_{(ad)} \xrightarrow{catalyst} Ba(NO_3)_2 \tag{26}$$

$$BaO + 2NO_{2(ad)} + O*_{(ad)} \xrightarrow{catalyst} Ba(NO_3)_2 \tag{27}$$

The increment of the input energy density has shown to enhance the NO_x storage capacity. For the PFC system, it is because more of the NO can be oxidized to NO_2 with the increase of input

energy density; hence more NO_2 may adsorb and form nitrate on the catalyst surface. For the PDC system, it is not only because of the higher NO oxidation to NO_2 in the gaseous phase but also due to more NO can be adsorbed onto the catalyst surface with the increase of input energy density as reported in the literature [24], and part of the adsorbed NO may react with the O-radical to form more NO_2; and thus the NO_2 may form more nitrates on the catalyst. Furthermore, the O-radical which is formed by the electron collisions with O_2 in the plasma may also increase with the increasing input energy density and thus more nitrites may oxidized directly by the O-radical to form more nitrate species on the catalyst surface. In this sense, it can explain why the nitrite species will decrease with the increasing of input energy density.

5. Conclusions

In this study, we presented the comparative assessment of NO_x storage capacity using PDC system, PFC system and catalyst-only. The plasma in the PDC system exhibited better promotional effect than the PFC system on the NO_x storage of $Pt/Ba/Al_2O_3$ catalyst as the NSC in PDC system increased by 25–91% whereas the NSC in the PFC system increased by 0.5–50% at the temperature range of 100–300 °C compared to the catalyst-only. The NO_x storage capacity of the catalyst increased with the increase of the input energy density both in the PDC and PFC system due to the higher NO oxidation at higher input energy density. Furthermore, more nitrates could be formed on the catalyst in both of the PDC and PFC system.

In the PFC system, the main role of plasma was to oxidize NO to NO_2 by the O-radical which was formed by the electron collisions with O_2 to facilitate the NO_x storage. In the PDC system, the plasma not only could increase the NO oxidation rate in the gaseous phase but also could enhance more NO to be absorbed onto the catalyst surface and may react with the O-radical to formed more NO_2, and thus promote the formation of nitrate on the catalyst. The results show that non-thermal plasma-assisted catalytic NO_x storage over $Pt/Ba/Al_2O_3$ may be an efficient and potential practical way to remove NO_x in lean burn engine.

Acknowledgements

The work was financially supported by National Natural Science Fund of China (Grant No. 20677034), and the National High-Tech Research and Development (863) Program of China (Grant Nos. 2006AA060301 and 2006AA06A304), and New Century Excellent Talents in University of China (NCET-05-078).

References

[1] N. Miyoshi, S. Matsumoto, K. Katoh, T. Tanaka, J. Harada, N. Takahashi, K. Yokota, M. Sugiara, K. Kasahara, SAE Technical Paper 950809 (1995) 1361.
[2] N. Takahashi, H. Shinjoh, T. Iijima, T. Suzuki, K. Yamazaki, K. Yokota, H. Suzuki, N. Miyoshi, S.-I. Matsumoto, T. Tanizawa, T. Tanaka, S.-S. Tateshi, K. Kasahara, Catal. Today 27 (1996) 63.
[3] L. Xu, G. Graham, R. McCabe, Catal. Lett. 115 (2007) 108.
[4] H. Mahzoul, J.F. Brilhac, P. Gilot, Appl. Catal. B 20 (1999) 47.
[5] F. Prinetto, G. Ghiotti, I. Nova, L. Lietti, E. Tronconi, P. Forzatti, J. Phys. Chem. B 105 (2001) 12732.
[6] C.M.L. Scholz, V.R. Gangwal, J.H.B.J. Hoebink, J.C. Schouten, Appl. Catal. B 70 (2007) 226.
[7] S. Kikuyama, I. Matsukuma, R. Kikuchi, K. Sasaki, K. Eguchi, Appl. Catal. A 226 (2002) 23.
[8] P.J. Schmitz, R.J. Baird, J. Phys. Chem. B 106 (2002) 4172.
[9] R.D. Clayton, M.P. Harold, V. Balakotaiah, Appl. Catal. B 81 (2008) 161.
[10] S. Salasc, M. Skoglundh, E. Fridell, Appl. Catal. B 36 (2002) 145.
[11] W.S. Epling, L.E. Campbell, A. Yezerets, N.W. Currier, J.E. Parks, Catal. Rev. 46 (2004) 163.
[12] J.Y. Luo, J.Y. Meng, Y.Q. Zha, Y.N. Xie, T.D. Hu, J. Zhang, T. Liu, Appl. Catal. B 78 (2008) 38.
[13] K.S. Kabin, R.L. Muncrief, M.P. Harold, Y. Li, Chem. Eng. Sci. 59 (2004) 5319.
[14] H. Miessner, K.-P. Francke, R. Rudolph, T. Hammer, Catal. Today 75 (2002) 325.
[15] J.V. Durme, J. Dewulf, C. Leys, H.V. Langenhove, Appl. Catal. B 78 (2008) 324.
[16] Y.S. Mok, J.H. Kim, S.W. Ham, I.-S. Nam, Ind. Eng. Chem. Res. 39 (2000) 3938.
[17] B. Eliasson, U. Kogelschatz, IEEE Trans. Plasma Sci. 19 (2) (1991) 309.
[18] Ch. Sedlmair, K. Seshan, A. Jentys, J.A. Lercher, J. Catal. 214 (2003) 308.
[19] P.T. Fanson, M.R. Horton, W.N. Delgass, J. Lauterbach, Appl. Catal. B 46 (2003) 393.
[20] B. Westerberg, E. Fridell, J. Mol. Catal. A: Chem. 165 (2001) 249.
[21] M. Saito, M. Sato, K. Sawada, J. Electrostat. 39 (1997) 305.
[22] M. Rickard, D. Rankin, F. Weinberg, F. Carleton, J. Electrostat. 63 (2005) 711.
[23] A. Labergue, L. Leger, E. Moreau, G. Touchard, J. Electrostat. 63 (2005) 961.
[24] H. Lin, Z. Huang, W.F. Shangguan, X.S. Peng, Proc. Combust. Inst. 31 (2007) 3335.
[25] Y.S. Mok, V. Ravi, H.C. Kang, B.S. Rajanikanth, IEEE Trans. Plasma Sci. 31 (2003) 157.
[26] R. Atkinson, D.L. Baulch, R.A. Cox, R.F. Hampson Jr., J.A. Kerr, J. Troe, J. Phys. Chem. Ref. Data 21 (1992) 1125.
[27] H. Mäzing, Advances in Chemical Physics, Wiley, New York, LXXX (1999) 315.
[28] Y.S. Mok, I. Nam, Chem. Eng. Technol. 22 (1999) 527.
[29] T. Hammer, T. Kishimoto, T. Miessner, R. Rudolph, SAE Paper 1999-01-3632 (1999) 1.
[30] L. Olsson, P. Jozsa, M. Nilsson, E. Jobson, Top. Catal. 42/43 (2007) 95.
[31] R.L. Muncrief, P. Khanna, K.S. Kabin, M.P. Harold, Catal. Today 98 (2004) 393.
[32] I. Nova, L. Lietti, L. Castoldi, E. Tronconi, P. Forzatti, J. Catal. 239 (2006) 244.
[33] W.S. Epling, L.E. Campbell, A. Yezerets, N.W. Currier, J.E. Park II, Catal. Rev. 46 (2004) 163.
[34] L. Lietti, P. Forzatti, I. Nova, E. Tronconi, J. Catal. 204 (2001) 175.
[35] E. Fridell, M. Skoglundh, B. Westerberg, S. Johansson, G. Smedler, J. Catal. 183 (1999) 196.